ALL REFRACTORY NbN/MgO/NbN TUNNEL JUNCTIONS

H.G. LeDuc*, J.A. Stern**, S. Thakoor*, and S.K. Khanna*
*Jet Propulsion Laboratory,
California Institute of Technology
4800 Oak Grove Dr.
Pasadena, CA. 91109
**California Institute of Technology
Pasadena, CA. 91125

ABSTRACT

We report the fabrication of all-refractory super-conductor-insulator-superconductor tunnel junctions of the form NbN/MgO/NbN. The MgO insulating barrier was deposited by e-beam evaporation. High quality junctions were fabricated with sum gaps of 5.2 meV, and a small subgap leakage parameter (V_m=30 mV, measured at 3mV). These devices are for eventual use as quasiparticle mixer elements in millimeter/submiltimeter wave heterodyne receivers. Fabrication techniques and current-voltage characteristics are discussed. We also propose a new growth mode for MgO films on NbN.

INTRODUCTION

Superconductor-Insulator-Superconductor (SIS) tunnel junctions have proven to be the most sensitive mixer elements for millimeter wave heterodyne receivers and are currently in use in several radio frequency astronomy observatories. (Reviews of SIS mixer applications, status, and theory can be found in refs.(1,2,3). More recently, the sensitivity of SIS tunnel junctions has been demonstrated in the submillimeter wave range to 450 GHz (4) and have the potential of being useful up to 1500 GHz. Therefore, SIS mixer elements are being developed for future submillimeter wave astronomy facilities, including NASA's proposed space based telescope (e.g., the Large Deployable Reflector). The exceptional mixing properties of SIS tunnel junctions are due to the strong nonlinearity in the tunneling current voltage characteristics which arises from the singularity in the quasiparticle density of states. Ideally, the width of the current onset at the superconducting energy gap (ΔV) is such that the condition for quantum detection ($\Delta V < h\nu/e$) is satisfied in the millimeter and submillimeter wave range. As a result, extremely sensitive receivers with low local oscillator power requirements become feasible. The responsivity of SIS quantum detectors is determined by the relative magnitudes of the photon assisted forward and reverse tunneling currents, with the maximum responsivity occurring when the reverse tunneling current is a minimum. For SIS junctions biased in the gap of the quasiparticle density of states, the reverse tunneling current is determined by the subgap leakage resistance which is historically expressed as $V_m = I_c R_{sg}$ where I_c is the Josephson critical current and R_{sg} is the subgap resistance measured at approximately half the gap (in our case 3 mV). The theoretical limit to the high frequency response of SIS junctions is a matter of conjecture, however, an upper limit occurs at photon energies for which tunneling can occur into the empty quasiparticle band in the reverse direction. The maximum cutoff frequency occurs when the junction is biased just below the current onset and is given by $f_m = 2\Delta_\Sigma/h$. A more immediate limit to high frequency response is the capacitive rolloff due to the junctions parallel capacitance (C) and normal tunneling

resistance (R_n). The tunneling parameters of interest include the sumgap (Δ_Σ), the subgap resistance parameter V_m, the width of the quasiparticle tunneling onset (ΔV), and the $R_n C$ product.

Current SIS mixer technology based on lead and lead alloy tunnel junctions suffers from materials problems associated with soft superconductors. These problems include poor thermal cycling characteristics, small superconducting energy gap, and low superconducting transition temperature ($T_c \approx 6$-$7°K$). Tunnel junctions based on all refractory, high transition temperature superconductors promise to provide solutions to these problems. In the past several years, NbN/MgO/NbN, SIS tunnel junctions have emerged as the most promising candidates to fulfill the requirements for practical receivers in the submillimeter wave range.

Niobium nitride in the B1 (NaCl) crystal structure has a T_c of approximately 16-17 K is refractory, mechanically robust, chemically stable and withstands thermal cycling well. The high T_c phase of NbN can be deposited by dc magnetron sputtering at substrate temperatures as low as room temperature (5). The refractory insulator, magnesium oxide (MgO), is also a B1 structure material with a lattice mismatch with NbN of approximately four per cent. There are conflicting reports in the literature concerning the growth mode of the MgO insulator on NbN, with Shoji et al. (6) reporting amorphous films and Talvacchio et al. (7) reporting epitaxial growth. In either case, there appears to be excellent materials compatibility between NbN and MgO. Both groups used rf-magnetron sputtering to deposit the MgO barrier, while in our work we have investigated the possibility of depositing MgO by electron beam evaporation. Since electron beam evaporation is a lower energy process than rf-sputtering, one might expect to produce less surface damage and higher quality insulating films. Our work has concentrated mainly on the development of techniques to fabricate high quality SIS tunnel junctions suitable for submillimeter wave mixer elements. In this paper we report our progress in this area, including the fabrication techniques and the current-voltage characteristics of NbN/MgO/NbN tunnel junctions with MgO deposited by electron beam evaporation. In addition, in the course of our work, we have obtained indirect evidence for a possible growth mode for MgO on NbN, and will discuss the implications of this mode for the fabrication of SIS junctions for high frequency mixer applications.

EXPERIMENTAL

The SIS trilayer is deposited completely in situ in an oil free ultra-high vacuum system (base pressure approximately 8 X 10^{-7} Pa). The NbN base and counter electrodes are deposited by dc reactive magnetron sputtering from a niobium target in an argon-nitrogen atmosphere. Typical sputtering parameters are: 10 cm target to substrate distance, 140 Watts sputtering power, 1.7 Pa argon partial pressure, and

0.23 Pa nitrogen partial pressure. The base and counter electrode thicknesses are approximately 350 and 200 nm respectively. Following the base electrode deposition, the vacuum chamber is evacuated in less than three minutes to 7×10^{-6} Pa and a MgO insulator barrier is deposited by electron beam evaporation. Barrier thicknesses are measured during deposition by a quartz crystal thickness monitor. An oxygen plasma was used as a post barrier deposition step to oxidize pinholes in the barrier. Two substrate heating modes were investigated. In the first mode the substrate temperature was maintained constant throughout the deposition process. In the second mode, the first 50 to 100 nm of the base electrode were deposited at a high substrate temperature followed by a gradual cool down to a lower temperature for the remainder of the deposition. In all cases a final layer of gold was deposited by electron beam evaporation to provide a contact surface, thus alleviating the need for special post process surface cleaning.

SIS tunnel junctions were fabricated by a method similar in detail to that described by Shoji et al. (8). The fabrication steps are shown schematically in figure (1). The junction area is masked using AZ4330 photoresist and standard photolithography. The device is delineated by etching the contact layer and counter electrode using reactive ion etching to form a mesa structure which defines the device area. The base electrode is then electrically isolated and the mesa planarized by thermally evaporating an SiO layer. Finally, the resist mask is lifted off and contacts thermally evaporated to complete the structure. The primary difference between our method and that of Shoji et al, is the addition of a dry etch step for the gold contact layer for which $CClF_3$ was used. Tunneling characteristics were determined from current-voltage (I-V) measurements taken at 4.2 K.
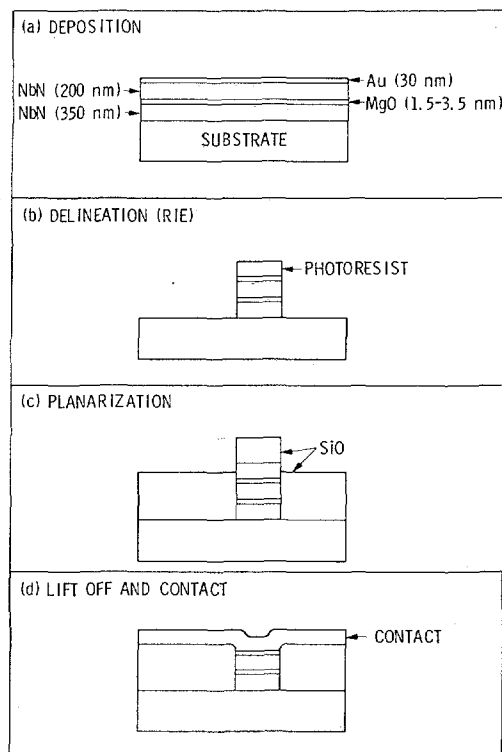

(a) DEPOSITION

NbN (200 nm) → Au (30 nm)
NbN (350 nm) → MgO (1.5-3.5 nm)
SUBSTRATE

(b) DELINEATION (RIE)

PHOTORESIST

(c) PLANARIZATION

SiO

(d) LIFT OFF AND CONTACT

CONTACT

Figure (1) Processing steps for SIS tunnel junctions.

RESULTS AND DISCUSSION

Figure (2) shows the I-V curves for SIS tunnel junctions using two different substrate heating sequences. In Figure (2a) the NbN/MgO/NbN trilayer was deposited with the substrates held at 210 C for the entire deposition. The average barrier thickness is approximately 2 nm and the junction area is 6 x 8 μm^2. The sum gap is $\Delta_\Sigma = 5.2$ meV, the width of the current onset at the gap is ΔV .8 meV, the subgap resistance parameter $V_m = 20$ mV, and the critical current density is $J_c = 1.0$ kA/cm^2. Because of the broad onset this junction would be unsatisfactory for operation as a quantum mixer below approximately 190 GHz. It is clear that the $R_n C$ product must be smaller, or V smaller or both before the quantum mixing properties of these devices can be tested. A large contribution to the gap width arises from averaging over lateral inhomogeneities in the superconducting films, such as mixed phases or the effects of crystal grain boundaries. Depositing the SIS trilayers at higher substrate temperatures may produce larger grain sizes and reduce the gap smearing. Attempts to deposit trilayers at higher temperatures yielded poor SIS junctions, with generally lower sum gaps and loss of barrier integrity. The source of these problems appears to be associated with high substrate temperatures during the barrier deposition and post barrier deposition oxygen pinhole cure. In figure (2b) is shown an SIS tunnel junction for which the base NbN electrode was deposited at 500 C for the first 100 nm, at which point the temperature was gradually lowered to 250 C for the remainder of the deposition. This procedure was motivated in part by the work of Gavaler et al. (9) in which it was shown that NbN homoepitaxy could take place at temperatures as low as 90 C. The initial high substrate temperature was introduced to nucleate large crystallites which could then be propagated at lower temperatures by homoepitaxy. The average barrier thickness is 2.5 nm and the device area is 6 x 8 μm^2. The sum gap, gap width, subgap leakage (V_m), and critical current density are 5.1 meV, 0.4 mV, 30 mV, and 0.7 kA/cm^2 respectively. The larger V_m and narrower gap represent significant improvements in device quality. Shown in figure (3) is the temperature dependance of the tunneling I-V characteristics for this junction. Little degradation in tunneling characteristics are observed at 8 K and the critical current is finite up to 15 K.

In our study we noticed an anomalous dependence of the tunneling resistance with barrier thickness. The tunneling resistances vary with MgO barrier thickness in our study slower than the theoretical exponential dependence. In addition, our tunneling resistances for a given barrier thickness are much smaller than the rf sputtered barriers of Shoji et al. (6). A possible explanation of this observation is that tunneling in e-beam deposited MgO barriers is dominated by areas which are thinner than the average barrier thickness measured by the in situ thickness monitor. We propose a new growth mode for MgO barriers on NbN. In contrast to the low substrate temperature rf-sputtered barriers of Shoji which are reported to be amorphous, we believe we are getting a polyepitaxial growth in which the first monolayer grows by planar epitaxy followed by nucleated island growth or the so called Stranski-Krastänov mechanism for epitaxy (10). This growth mode occurs when the deposit (MgO) has a lower surface energy than the substrate (NbN) so that the lowering of surface energy can dominate any strain energy induced by lattice mismatch (4 per cent mismatch for NbN/MgO). The second monolayer cannot lower the surface energy any further and nucleated island growth occurs to minimize the strain energy. This mode of growth is supported
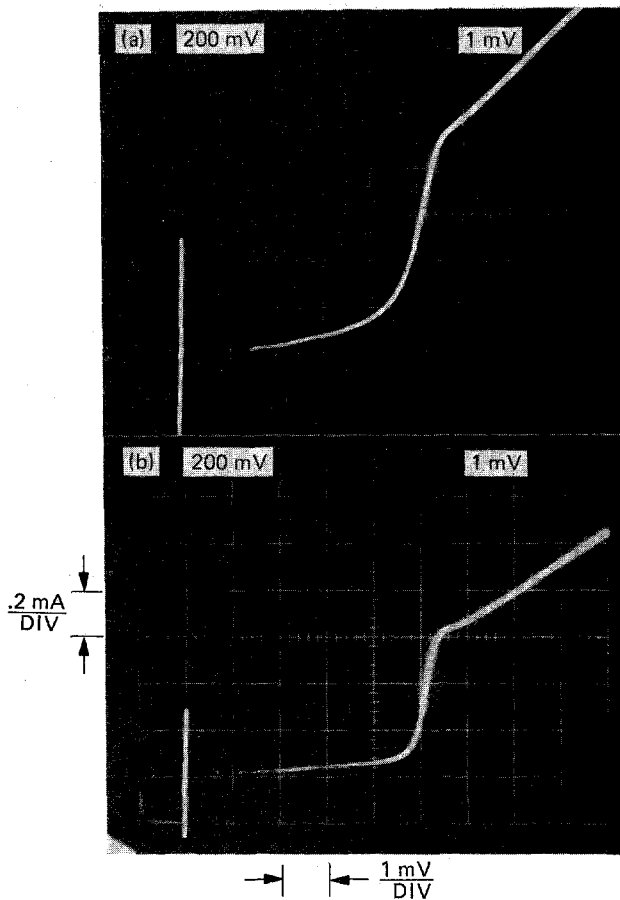
Figure (2) I-V curves for two NbN./MgO/NbN tunnel junctions prepared using different substrate heating sequences (a)(substrates held at 210C throughout deposition (b) substrates held at 500C for first 10 nm of depostion and lowered gradually to 250C for the barrier and counter electrode deposition.
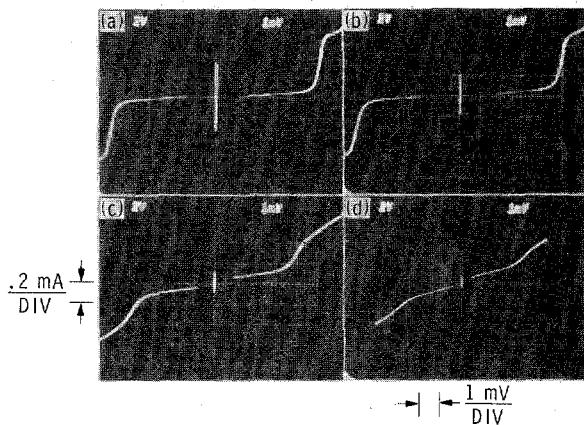

Figure (3) I-V curves for the NbN/MgO/NbN tunnel junction shown in Figure (1b) measured at various junction temperatures (a) 4.2K (b) 8K (c) 13K (d) 15K

indirectly by the work of Talvacchio et al. (7) in which rf-sputtered MgO barriers on high temperature substrates were observed by RHEED to be epitaxial, however diffuse diffraction spots in LEED were observed leading the authors to conclude that the MgO films were rough. The weak thickness dependence of tunneling resistance would be explained in this model

since the monolayer regions would dominate the tunneling properties and increasing the barrier thickness would merely decrease the area of these regions. This decrease in area would lead to an increase in tunneling resistance which would have a weaker dependence on barrier thickness than the exponential dependence expected for uniform barriers. The implications for SIS device development is that ultimately barriers as thin as a monolayer may be possible in the NbN/MgO system leading to tunnel junctions with the highest speed (the smallest RnC product) that can be realized with these materials. Work is currently in progress to obtain more direct evidence for this growth mode.

CONCULSIONS

We have fabricated high quality NbN/MgO/NbN, SIS tunnel junctions with MgO deposited by e-beam evaporation. Tunneling characteristics include large sum gaps (as large as $\Delta_\Sigma \approx 5.2$ meV), small subgap leakages ($V_m \approx 30$mV), small quasiparticle onset widths ($V \approx 0.4$mV) and large critical current densities (maximum J_c 3.0kA/cm^2). The temperature dependence of the I-V characteristics indicate little degradation up to 8 K and definite SIS behavior up to 15 K. Finally, data suggest that the growth of MgO on NbN is occurring according to the Stranski-Krastánov mechanism.

REFERENCES

1   Paul L. Richards, Physics Today 39(3),54 (1986)

2.   T.G. Philips and D.P. Woody, Ann. Rev. Astron. Astrophys. 20,285 (1982)

3.   J.R. Tucker and M.J. Feldman, Rev. Modern Phys. 57,1055 (1985)

4.   M.J. Wengler, D.P. Woody, R.E. Miller, and T.G. Phillips, International Journal of Infrared and Millimeter Waves, 6,697 (1985)

5.   S. Thakoor, J.L. Lamb, A.P. Thakoor, and S.K. Khanna, J. Appl. Phys. 58(12),4643 (1985)

6.   A. Shoji, M. Aoyagi, S. Kosaka, F. Shinoki, and H. Hayakawa Appl. Phys. Lett. 46(11),1098 (1985)

7.   J. Talvacchio, A.I. Braginski, M.A. Janocko, and J.R. Gavaler, Bulletin of the American Physical Society 31(3),438 (1986)

8.   A. Shoji, F. Shinoki, S. Kosaka, M. Aoyagi, and H. Hayakawa, Appl. Phys. Lett. 41,1097 (1982)

9.   J.R. Gavaler, J. Talvacchio, and A.I. Braginski, to be published in Advances in Cryogenic Engineering-Materials, ed. A. F. Clark and R.P. Reed (Plenum,New York)

10. E. Bauer and H. Poppa, Thin Solid Films 12,167 (1972)